Chiral phase transition of QCD at finite temperature and density from the Schwinger-Dyson equation

Masayasu Harada*
Department of Physics and Astronomy, University of North Carolina, Chapel Hill, North Carolina 27599-3255

Akihiro Shibata†
Computing Research Center, High Energy Accelerator Research Organization (KEK), Tsukuba 305-0181, Japan
(Received 17 July 1998; published 23 November 1998)

We study the chiral phase transition of QCD at finite temperature and density by numerically solving the Schwinger-Dyson equation for the quark propagator with the improved ladder approximation in the Landau gauge. Using the solution we calculate a pion decay constant from a generalized version of the Pagels-Stokar formula. The chiral phase transition point is determined by analyzing an effective potential for the quark propagator. We find solutions for which chiral symmetry is broken while the value of the effective potential is larger than that for the chiral symmetric vacuum. These solutions correspond to metastable states, and the chiral symmetric vacuum is energetically favored. We present a phase diagram on the general temperature-chemical potential plane, and show that phase transitions are of first order in wide range.
[S0556-2821(98)04923-6]

PACS number(s): 12.38.Lg, 11.10.Wx, 11.30.Rd

I. INTRODUCTION

In QCD an approximate chiral symmetry exists at the Lagrangian level and it is spontaneously broken by the strong gauge interaction. Accordingly approximate Nambu-Goldstone (NG) bosons appear, and pions are regarded as NG bosons. In hot and/or dense matter, however, quark condensates melt at some critical point, and chiral symmetry is restored (for recent reviews, see, e.g., Ref. [1]). To study the chiral phase transition we need a nonperturbative treatment.

The Schwinger-Dyson equation (SDE) is a powerful tool for studying the qualitative structure of the chiral symmetry breaking of QCD. By suitable choices of the running coupling, in which the asymptotic freedom is incorporated, the SDE provides a nontrivial solution for the mass function. The behavior of the mass function at high energy is consistent with that given by the operator product expansion technique (for a review, see, e.g., Ref. [2]). The SDE is understood as a stationary condition of an effective potential for the quark propagator, and the chiral broken solution is energetically favored by the effective potential [3–6].

The SDE was applied for studying the chiral phase transition of QCD at finite temperature and/or density [7–18]. In many of those the chiral phase transition point was determined from the point where the mass function (or pion decay constant) vanished without studying an effective potential. In Ref. [13] an effective potential for the mass function was analyzed by using an approximate form of the momentum dependence of the mass function. It was shown that there were metastable states where chiral symmetry was broken while the energy was bigger than that for the symmetric vacuum. It is interesting to study whether this kind of metastable state is derived by fully solving the SDE.

In this paper we study the chiral phase transition in QCD at finite temperature and/or density by numerically solving the SDE using the Matsubara formalism. As an order parameter we calculate the pion decay constant using a generalized version of the Pagels-Stokar formula [19]. We calculate the value of the effective potential at the solution of the SDE to determine the chiral phase transition points. We show that metastable states actually exist in a wide range. The order of the phase transitions is determined by comparing the order parameter with the effective potential. The phase transition is of first order for a wide range at $T \neq 0$ and $\mu \neq 0$.

This paper is organized as follows. An effective potential for the quark propagator is introduced at finite temperature and/or density in Sec. II. The SDE is derived as a stationary condition of the potential. In Sec. III a formula for calculating the pion decay constant is presented. Section IV is the main part of this paper, where numerical solutions of the SDE are shown. Values of the pion decay constant and the effective potential are calculated from the solutions, and the phase structure is studied. Finally a summary and discussion are given in Sec. V.

II. EFFECTIVE POTENTIAL AND SCHWINGER-DYSON EQUATION

At zero temperature the effective action for the quark propagator S_F is given by [4,6]

$$\Gamma[S_F] = i\,\mathrm{Tr}\ln S_F - \mathrm{Tr}[i\partial\!\!\!/ S_F] - i\kappa_{\mathrm{2PI}}[S_F], \qquad (2.1)$$

where κ_{2PI} stands for the two-particle-irreducible (with respect to the quark line) diagram contribution. In this paper we take a first order approximation for κ_{2PI}, in which the one-gluon exchange graph contributes:

*Electronic address: harada@physics.unc.edu. Present address: Department of Physics, Nagoya University, Nagoya 464-8602, Japan.
†Electronic address: ashibata@post.kek.jp

$$\kappa_{2\mathrm{PI}}[S_F] = -\frac{N_f N_C C_2}{2}\int d^4x d^4y g^2 \times \mathrm{tr}[S_F(x-y) i\gamma_\mu S_F(y-x) i\gamma_\nu] D^{\mu\nu}(x-y), \tag{2.2}$$

where the number of flavor (N_f) and of color (N_C) and the second Casimir coefficient of SU(N_C) (C_2) appear since we factor color and flavor indices from the quark and gluon propagators. In this expression, the quark propagator S_F carries bispinor indices and the gluon propagator $D^{\mu\nu}$ carries Lorenz indices. From the above effective action the effective potential for S_F is obtained by the usual procedure. In momentum space it is expressed as

$$V[S_F] = \int \frac{d^4p}{i(2\pi)^4}\{\ln\det[S_F(p)] + \mathrm{tr}[\not{p} i S_F(p)]\} + \frac{1}{2}\int \frac{d^4p}{i(2\pi)^4}\int \frac{d^4k}{i(2\pi)^4} C_2 g^2(p,k) \times \mathrm{tr}[i S_F(p)\gamma_\mu i S_F(k)\gamma_\nu] i D^{\mu\nu}(k-p), \tag{2.3}$$

where an overall factor $N_C N_f$ is dropped. The running coupling $g^2(p,k)$ is introduced to improve the SDE to include the aymptotic freedom of QCD. An explicit form of the running coupling will be given below. In this paper we take the Landau gauge for the gluon propagator:

$$iD^{\mu\nu}(l) = \frac{1}{l^2}\left[g^{\mu\nu} - \frac{l^\mu l^\nu}{l^2}\right]. \tag{2.4}$$

The general form of the full quark propagator is expressed as

$$iS_F^{-1}(p) = A(p)\not{p} - B(p). \tag{2.5}$$

The SDE for the quark propagator S_F is given as a stationary condition of the above effective potential [4] (see also, Ref. [6]). The SDE gives coupled equations for A and B. If the running coupling $g(p,k)$ is a function in p^2 and k^2, i.e., if it does not depend on $p\cdot k$, it is easy to show that $A(p^2)=1$ is a solution of the SDE in the Landau gauge with the ladder approximation.

Let us go to nonzero temperature and density. In the imaginary time formalism [20] the partition function is calculated by the action given by (see, for reviews, e.g., Refs. [21,22])

$$S = \int_0^{1/T} d\tau \int d^3x [\mathcal{L}_{\mathrm{QCD}} + \mu\bar{\psi}\gamma^0\psi], \tag{2.6}$$

where T and μ denote the temperature and chemical potentials associated with the quark (baryon) number density, and $\mathcal{L}_{\mathrm{QCD}}$ takes the same form as the QCD Lagrangian at $T=\mu=0$. From the above action we obtain an effective potential for the quark propagator S_F similar to the one in Eq. (2.3):

$$V[S_F] = T\sum_u \int \frac{d^3\vec{p}}{(2\pi)^3}\{\ln\det[S_F(p)] + \mathrm{tr}[\not{p} i S_F(p)]\} + \frac{1}{2}T^2\sum_{u,v}\int \frac{d^3\vec{p}}{(2\pi)^3}\int \frac{d^3\vec{k}}{(2\pi)^3} C_2 g^2(p,k) \times \mathrm{tr}[i S_F(p)\gamma_\mu i S_F(k)\gamma_\nu] i D^{\mu\nu}(k-p), \tag{2.7}$$

where

$$p_0 = iu + \mu, \quad u = (2m+1)\pi T, \qquad k_0 = iv + \mu, \quad v = (2n+1)\pi T \quad (n,m = \text{integer}), \tag{2.8}$$

and Σ_u and Σ_v imply summations over m and n, respectively.

The argument of the running coupling should be taken as $(k-p)^2$ for preserving chiral symmetry [23]. However, as is shown in Ref. [23], the angular average, i.e., where the running coupling is a function in $-p_0^2+|\vec{p}|^2-k_0^2+|\vec{k}|^2$, is a good approximation at $T=\mu=0$. If we naively extend this approximation, the running coupling will depend on μ. However, the running coupling should not depend on μ. Then in this paper we use the approximation where the running coupling is a function in $-(p_0-\mu)^2+|\vec{p}|^2-(k_0-\mu)^2+|\vec{k}|^2$. The explicit form of the running coupling is [24]

$$g^2(p,k) = (4\pi)^2\frac{3}{11N_C - 2N_f}\bar{\lambda}\left[\ln\left(\frac{u^2+x^2+v^2+y^2}{\Lambda_{\mathrm{qcd}}^2}\right)\right],$$

$$\bar{\lambda}(t) = \begin{cases} \dfrac{1}{t} & \text{if } t_F < t, \\ \dfrac{1}{t_F} + \dfrac{(t_F-t_C)^2-(t-t_C)^2}{2t_F^2(t_F-t_C)} & \text{if } t_C < t < t_F, \\ \dfrac{1}{t_F} + \dfrac{(t_F-t_C)}{2t_F^2} & \text{if } t < t_C, \end{cases} \tag{2.9}$$

with

$$x \equiv |\vec{p}|, \quad y \equiv |\vec{k}|. \tag{2.10}$$

Λ_{qcd} is a scale where the one-loop running coupling diverges, and the value of Λ_{qcd} will be determined later from the infrared structure of the present analysis.[1] t_F and t_C are parameters introduced to regularize the infrared behavior of the running coupling. In the numerical analysis below, since the dominant part of the mass function lies below the threshold of charm quark, we will take $N_f=3$ and $N_C=3$. Moreover, we use fixed values $t_F=0.5$ and $t_C=-2.0$ [2].

[1]The usual Λ_{QCD} is determined from the ultraviolet structure.

The general form of the full quark propagator, which is invariant under the parity transformation, is given by [7,11,12,15]

$$iS_{\mathrm{F}}^{-1}(p)=A(p)\not{p}-B(p)+C(p)p_0\gamma^0-\frac{i}{2}[\gamma^0,\not{p}]D(p). \tag{2.11}$$

Here $A\sim D$ are functions in p_0 and $|\vec{p}|$ (as well as T and μ), although we write $A(p)$, etc.

It should be noticed that the effective potential in Eq. (2.7) is invariant under the tranfromation

$$S_F(p_0,\vec{p})\to S_F'(p_0,\vec{p})=(i\gamma^1\gamma^3\gamma^0)S_F^T(p_0,-\vec{p})(i\gamma^0\gamma^1\gamma^3), \tag{2.12}$$

where S_F^T implies transposition of S_F in spinor space.[2] At $T=\mu=0$ this is nothing but the time reversal symmetry. It is natural to expect that this ''time reversal'' symmetry is not spontaneously broken. The existence of this ''time reversal'' leads to $D(p)=0$.

Moreover, at $\mu=0$ the effective potential is invariant under the following ''charge conjugation:''

$$S_F(p)\to S_F'(p)=-(i\gamma^2\gamma^0)S_F^T(-p)(i\gamma^2\gamma^0). \tag{2.13}$$

We also assume that this symmetry is not spontaneously broken, and it implies that all the scalar functions A, B, and C (as well as D) are even functions in $p_0=iu$. As we mentioned above, at $T=\mu=0$, of course $C(p)=0$, and $A(p)=1$ in the Landau gauge. $C(p)\neq 0$ as well as $A(p)\neq 1$ does not imply chiral symmetry breaking, and nonzero $B(p)$ is the only signal of breaking in the present analysis. Then we consider $A(p)-1=C(p)=0$ as an approximate solution at general T and μ. We note that a nonzero $D(p)$ also breaks chiral symmetry; however, this term does not contribute to the local order parameter of chiral symmetry, $\langle\bar{\psi}\psi\rangle=-\int \mathrm{tr}\, S_F$. We choose a vacuum of ''time reversal'' invariance as discussed above.[3]

As in the case at $T=\mu=0$, the SDE is given as a stationary condition of the effective potential (2.7):

$$iS_{\mathrm{F}}^{-1}(p)-\not{p}=T\sum_v \int\frac{d^3\vec{k}}{(2\pi)^3}C_2g^2(p,k)\gamma_\mu iS_{\mathrm{F}}(k_f)\times\gamma_\nu iD^{\mu\nu}(k-p). \tag{2.14}$$

By taking a trace and performing the three-dimensional angle integration (note that the present form of the running coupling does not depend on the angle), we obtain a self-consistent equation for B:

$$B(p)=K(p,k)*\frac{B(k)}{B^2(k)-k^2}\equiv T\sum_v\int\frac{dyy^2}{2\pi^2}K(p,k)\frac{B(k)}{B^2(k)-k^2}, \tag{2.15}$$

where

$$K(p,k)\equiv\frac{3}{2}C_2g^2(p,k)\frac{1}{2xy}\ln\left(\frac{(u-v)^2+(x+y)^2}{(u-v)^2+(x-y)^2}\right). \tag{2.16}$$

In general cases B is a complex function. By using the fact that $K(p,k)$ is a real function, it is easily shown that $B^*(p)$ satisfies the same equation as $B(p^*)$ does, where $p^{*\mu}=(p^{0*},\vec{p})=(-iu+\mu,\vec{p})$. So these two are equal to each other up to a sign, $B^*(p)=B(p^*)$ or $B^*(p)=-B(p^*)$. Since B is an even function in p_0 at $\mu=0$, the choice of positive (negative) sign implies that B is real (pure imaginary) at $\mu=0$. Here B should be real at $\mu=0$; then,

$$B^*(p)=B(p^*). \tag{2.17}$$

After a solution of the SDE (2.14) is substituted with the approximate solution $A(p)-1=C(p)=0$ into Eq. (2.7), the effective potential becomes

$$\overline{V}[B_{\mathrm{sol}}]\equiv V[B_{\mathrm{sol}}]-V[B=0]=\frac{2}{\pi^2}T\sum_u\int dxx^2\left[-\ln\left(\frac{B_{\mathrm{sol}}^2(p)-p^2}{-p^2}\right)+\frac{B_{\mathrm{sol}}^2(p)}{B_{\mathrm{sol}}^2(p)-p^2}\right], \tag{2.18}$$

where B_{sol} denotes a solution of Eq. (2.15). This value of the effective potential is understood as the energy density of the solution. So the true vacuum should be determined by studying the value of the effective potential. When the value of $\overline{V}[B_{\mathrm{sol}}]$ for a nontrivial solution B_{sol} is negative, the chiral broken vacuum is energetically favored. Positive $\overline{V}[B_{\mathrm{sol}}]$, however, implies that the chiral symmetric vacuum is a true vacuum.

III. PION DECAY CONSTANT

At zero temperature and zero chemical potential the pion decay constant is defined by the matrix element of the axial-vector current between the vacuum and one-pion state:

$$\langle 0|J_{5\mu}^a(0)|\pi^b(q)\rangle=i\delta^{ab}q_\mu f_\pi, \tag{3.1}$$

where a and b denote isospin indices and $J_{5\mu}^a=\bar{\psi}\gamma_\mu\gamma_5T^a\psi$ is an axial-vector current with T^a being a generator of SU(N_{f}). At finite temperature and density there are two distinct pion decay constants [25] according to space-time symmetry of the matrix element, which are defined by

[2] In our convention, $(\gamma^0)^*=\gamma^0$, $(\gamma^1)^*=\gamma^1$ and $(\gamma^3)^*=\gamma^3$, while $(\gamma^2)^*=-\gamma^2$.

[3] Actually, in the numerical calculation of the SDE in a bifurcation approximation, no $D(p)\neq 0$ solution is obtained.

$$\langle 0|J^a_{5\mu}(0)|\pi^b(q)\rangle_{T,\mu} = i\delta^{ab}[V_\mu(V\cdot q)f_{\pi L}+(g_{\mu\nu}-V_\mu V_\nu)q^\nu f_{\pi T}], \tag{3.2}$$

where $V^\mu=(1,\vec{0})$ is a vector of the medium. In this expression $f_{\pi L}$ and $f_{\pi T}$ are defined in the zero-momentum limit $q\to 0$ [25].

The above pion decay constants are expressed by using the amputated pion Bethe-Salpeter (BS) amplitude $\hat{\chi}$ as

$$V_\mu(V\cdot q)f_{\pi L}+(g_{\mu\nu}-V_\mu V_\nu)q^\nu f_{\pi T} = -\frac{N_C}{2}T\sum_u \int \frac{d^3p}{(2\pi)^3} \times \mathrm{tr}[\gamma_\mu\gamma_5 iS_F(p+q/2)\hat{\chi}(p;q)iS_F(p-q/2)]. \tag{3.3}$$

By using current conservation, it is shown that the pion momentum $\vec{q}$ and the pion energy q_0 satisfy the dispersion relation [25]

$$q_0^2=\frac{f_{\pi T}}{f_{\pi L}}|\vec{q}|^2. \tag{3.4}$$

It is straightforward to obtain the pion decay constant if we have an explicit expression of the amputated pion BS amplitude. Although it is generally quite difficult to obtain the BS amplitude, one can determine it in the $q\to 0$ limit $\hat{\chi}(p;q=0)$ from the chiral Ward-Takahashi identity

$$iq^\mu\Gamma^a_{5\mu}(p-q/2,p+q/2) = S_F^{-1}(p-q/2)T_a\gamma_5+T_a\gamma_5 S_F^{-1}(p+q/2), \tag{3.5}$$

where $\Gamma^a_{5\mu}$ is the axial-vector–quark–antiquark vertex function, and we have suppressed color indices. [Note that q^0 in Eq. (3.5) is independent of $\vec{q}$; i.e., they do not generally satisfy the pion on-shell dispersion relation (3.4).] In the zero-momentum limit $\vec{q}$, $q^0\to 0$ (the on-shell limit of the pion), $\Gamma^a_{5\mu}$ is dominated by the pion-exchange contribution

$$i\Gamma^a_{5\mu}(p-q/2,p+q/2) \underset{\vec{q},q^0\to 0}{\to} i[V_\mu(V\cdot q)f_{\pi L}+(g_{\mu\nu}-V_\mu V_\nu)q^\nu f_{\pi T}] \times\frac{1}{q_0^2-\omega_q^2}\hat{\chi}(p,0)T_a, \tag{3.6}$$

where $\omega_q^2=(f_{\pi T}/f_{\pi L})|\vec{q}|^2$. Substituting Eq. (3.6) into Eq. (3.5) and taking the zero-momentum limit, we find

$$\hat{\chi}(p;0)=\frac{2}{f_{\pi L}}B(p)\gamma_5, \tag{3.7}$$

where we have used $D(p)=0$ in $S_F(p)$.

The approximation adopted by Pagels and Stokar [19] essentially neglects derivatives of $\hat{\chi}$ in the zero-momentum limit (see, for reviews, e.g., Refs. [2,26]):

$$\lim_{\vec{q}\to 0}\frac{\partial}{\partial|\vec{q}|}\hat{\chi}(p;q)=\lim_{\vec{q}\to 0}\frac{\partial}{\partial q_0}\hat{\chi}(p;q)=0. \tag{3.8}$$

This approximation is the same as replacing $\hat{\chi}(p;q)$ in Eq. (3.3) with $\hat{\chi}(p;0)$, and reproduces the exact value of f_π at $T=0$ in the ladder approximation within a small error [2]. Then we use the same approximation at finite T and μ in this paper. Replacing $\hat{\chi}(p;q)$ with $\hat{\chi}(p;0)$ in Eq. (3.3), differentiating Eq. (3.3) with respect to q^α, and taking $q\to 0$ limit, we obtain

$$i\delta^{ab}[V_\mu V_\alpha f_{\pi L}+(g_{\mu\alpha}-V_\alpha V_\mu)f_\pi] = -\frac{N_C}{2}T\sum_u\int\frac{d^3p}{(2\pi)^3}\mathrm{tr}\left[\gamma_\mu\gamma_5\left\{\frac{i}{2}\frac{S_F(p)}{\partial p^\alpha}\hat{\chi}(p;0)iS_F(p) + iS_F(p)\hat{\chi}(p;0)\frac{i}{2}\frac{S_F(p)}{\partial p^\alpha}\right\}\right]. \tag{3.9}$$

Here we have incorporated the on-shell dispersion relation (3.4). Then substituting Eq. (3.7) into Eq. (3.9) and taking the $V_\mu V_\alpha$ part, we find

$$f_{\pi L}^2=4N_C T\sum_u\int\frac{dx x^2}{2\pi^2}\frac{B(p)\left(B(p)-p_0\frac{\partial B(p)}{\partial p_0}\right)}{(B^2(p)-p^2)^2}, \tag{3.10}$$

where we performed a three-dimensional angle integration. If the mass function $B(p)$ is a function in $p^2=p_0^2-\vec{p}^2$, this agrees with the formula derived in Ref. [14]. We also obtain a similar formula for $f_{\pi T}$ by selecting the $(g_{\mu\alpha}-V_\mu V_\alpha)$ part:

$$f_{\pi T}f_{\pi L}=4N_C T\sum_u\int\frac{dx x^2}{2\pi^2}\frac{B(p)\left(B(p)-\frac{x}{3}\frac{\partial B(p)}{\partial x}\right)}{(B^2(p)-p^2)^2}, \tag{3.11}$$

where $f_{\pi L}$ on the left hand side appears from the normalization of $\hat{\chi}$ (see Eq. (3.7)).

It is convenient to define a space-time averaged pion decay constant by

$$f_\pi^2\equiv f_{\pi L}\frac{1}{4}g^{\mu\alpha}\frac{\partial}{\partial q^\alpha}[V_\mu(V\cdot q)f_{\pi L}+(g_{\mu\nu}-V_\mu V_\nu)q^\nu f_{\pi T}] = \frac{1}{4}(f_{\pi L}^2+3f_{\pi T}f_{\pi L}). \tag{3.12}$$

This expression agrees with Pagels-Stokar formula [19] at $T=0$ and $\mu=0$ after replacing the integral variables.

In the formula (3.10) we need a derivative of $B(p)$ with respect to p_0. However, what is obtained by solving the SDE

(2.15) is a function in discrete $u=(2n+1)\pi T$. To obtain the derivative an ''analytic continuation'' in u from a discrete variable to a continuous variable is needed. This ''analytic continuation'' is done by using the SDE (2.15) itself:

$$p_0\frac{\partial B(p)}{\partial p_0}=p_0\frac{\partial K(p,k)}{\partial p_0}\frac{B(k)}{B^2(k)-k^2}. \tag{3.13}$$

IV. NUMERICAL ANALYSIS

In this section we will numerically solve the SDE (2.15) and calculate the effective potential and the pion decay constant $f_\pi(T)$ defined in Eq. (3.12) for the cases (1) $T=0$ and $\mu\neq 0$, (2) $T\neq 0$ and $\mu=0$, and (3) $T\neq 0$ and $\mu\neq 0$, separately. The essential parameters in the present analysis are $\Lambda_{\rm qcd}$ and t_F in the running coupling (2.9). In this paper we fix $t_{\rm F}=0.5$ and the value of $\Lambda_{\rm qcd}$ is determined by calculating the pion decay constant through the Pagels-Stokar formula [19] at $T=\mu=0$. Most results are presented by the ratio to pion decay constant at $T=\mu=0$. When we present actual values, we use the value of the pion decay constant in the chiral limit, $f_\pi=88$ MeV [27]. (This value of f_π yields $\Lambda_{\rm qcd}\simeq 582$ MeV.)

A. Preliminary

Here we will summarize the framework of the numerical analysis done below. Variables x and y in Eq. (2.10) take continuous values from 0 to ∞. To solve the SDE numerically we first introduce new variables X and Y as $X\equiv\ln(x/\Lambda_{\rm qcd})$ and $Y\equiv\ln(y/\Lambda_{\rm qcd})$. These variables take values from $-\infty$ to ∞. Dominant contributions to the decay constant and the effective potential lie around 0; i.e., x or y is around $\Lambda_{\rm qcd}$, as shown later. Then we introduce ultraviolet and infrared cutoffs $X,Y\in[\lambda_{\rm IR},\lambda_{\rm UV}]$. Finally, we descretize X and Y at N_X points evenly:

$$X_i,Y_i=\lambda_{\rm IR}+\Delta X\cdot i,\quad i=0,1,\ldots,N_X-1,$$

$$\Delta X=\frac{\lambda_{\rm UV}-\lambda_{\rm IR}}{N_X-1}. \tag{4.1}$$

Accordingly integrations over x and y are replaced with appropriate summations

$$\int dx,\int dy\to\Delta X\sum_i e^{X_i},\ \Delta X\sum_i e^{Y_i}. \tag{4.2}$$

We extract the derivative of $B(p)$ with respect to x, which is used in the formula for $f_{\pi T}$ in Eq. (3.11), from three points by using a numerical differentiation formula:

$$x\frac{\partial B(x)}{\partial x}\bigg|_{x/\Lambda_{\rm qcd}=e^{X_i}}\simeq\frac{4B(x_{i+1})-3B(x_i)-B(x_{i+2})}{2\Delta X}. \tag{4.3}$$

In the case of $T=0$ the Matsubara frequency sum becomes an integration over u or v from $-\infty$ to ∞. By using the property (2.17) we can restrict this region from 0 to ∞. Then we will perform a procedure similar to that for x and y:

$$U_n=\ln(u_n/\Lambda_{\rm qcd}),\quad V_n=\ln(v_n/\Lambda_{\rm qcd})=\Lambda_{\rm IR}+\Delta U\cdot n,$$
$$n=0,1,\ldots,N_U-1,\quad \Delta U=\frac{\Lambda_{\rm UV}-\Lambda_{\rm IR}}{N_U-1}. \tag{4.4}$$

In the case of $T\neq 0$ we truncate the infinite sum of the Matsubara frequency at a finite number N_U:

$$\sum_{n=-\infty}^{\infty}\to\sum_{n=-N_U-1}^{N_U}. \tag{4.5}$$

The above Eqs. (4.1)–(4.5) set the regularizations adopted in this paper. We will check that the results are independent of the regularizations.

Solving the SDE is done by an iteration method:

$$B_{\rm new}(p)=K(p,k)\frac{B_{\rm old}(k)}{B^2_{\rm old}(k)-k^2}. \tag{4.6}$$

Starting from a trial function, we stop the iteration if the following condition is satisfied:

$$\varepsilon\Lambda_{\rm qcd}^6>\frac{1}{4}{\rm tr}\left[\left(\frac{\delta V}{\delta[S_F(p)]_{\rm old}}\right)^\dagger\left(\frac{\delta V}{\delta[S_F(p)]_{\rm old}}\right)\right]$$
$$=[B_{\rm old}(p)-B_{\rm new}(p)]^\dagger[B_{\rm old}(p)-B_{\rm new}(p)], \tag{4.7}$$

with suitably small ε. To obtain the second line we have used the fact that $A(p)-1=C(p)=0$ is an approximate solution. This condition is natural in the sense that the stationary condition of the effective potential is satisfied within a required error. In this paper we use $\varepsilon=10^{-10}$.

B. $T=0$ and $\mu\neq 0$

As we discussed in the previous subsection the infinite Matsubara frequency sum becomes an integration over the continuous variable u or v at $T=0$. Descretizations of these variables as well as x and y are done as in Eqs. (4.1) and (4.4). We use the following choice of infrared and ultraviolet cutoffs:

$$X,Y\in[-4.9,2.9],$$
$$U,V\in[-10.0,2.8]. \tag{4.8}$$

For initial trial functions we use the following two types:

$$\text{(A)}\quad B(p)=B_{\rm sol}(p)|_{T=\mu=0},$$
$$\text{(B)}\quad B(p)=\begin{cases}0.1\Lambda_{\rm qcd} & \text{for } U_n\leqslant U_{20} \text{ and } X_i\leqslant X_{10},\\ 0 & \text{otherwise,}\end{cases} \tag{4.9}$$

where $B_{\rm sol}(p)|_{T=\mu=0}$ is a solution of the SDE at $T=\mu=0$, and U_n and X_i are descretized variables as in Eqs. (4.1) and

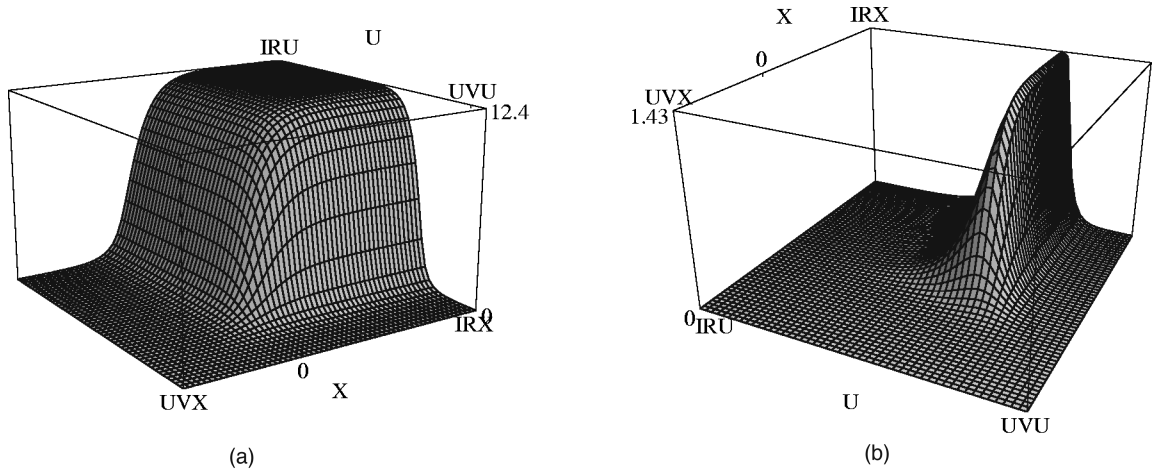

FIG. 1. Solution of the SDE at $\mu/f_\pi=0.3$ for $N_U=70$, $N_X=60$: (a) real part, (b) imaginary part. The scale $\Lambda_{\rm qcd}$ is indicated by 0 on U and X axes. Each number on the top of the vertical axis is the maximum value of $\mathrm{Re}\,B/f_\pi$ or $\mathrm{Im}\,B/f_\pi$.

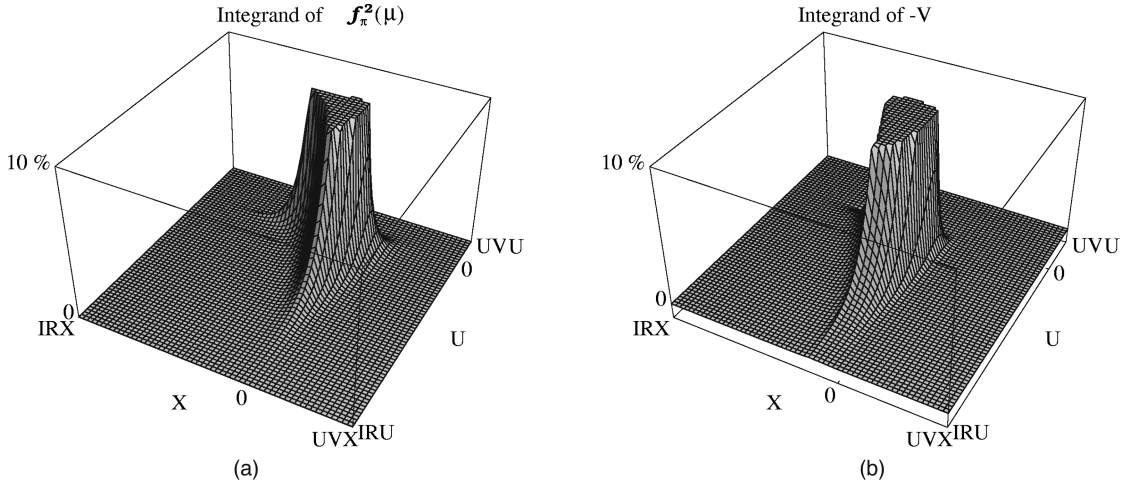

FIG. 2. Integrands of (a) $f_\pi^2(\mu)$ and (b) $-\overline{V}[B_{\rm sol}]$ at $\mu/f_\pi=0.3$ for $N_U=70$, $N_X=60$. The upper 9/10 of each figure is clipped.

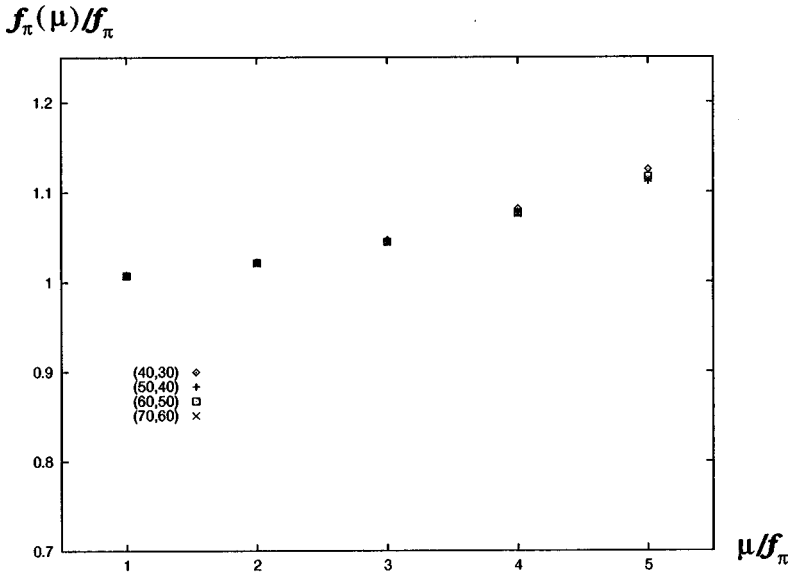

FIG. 3. Typical values of $f_\pi(\mu)/f_\pi$ for four choices of the size of descretization, $(N_U,N_X)=(40,30)$, (50,40), (60,50), and (70,60).

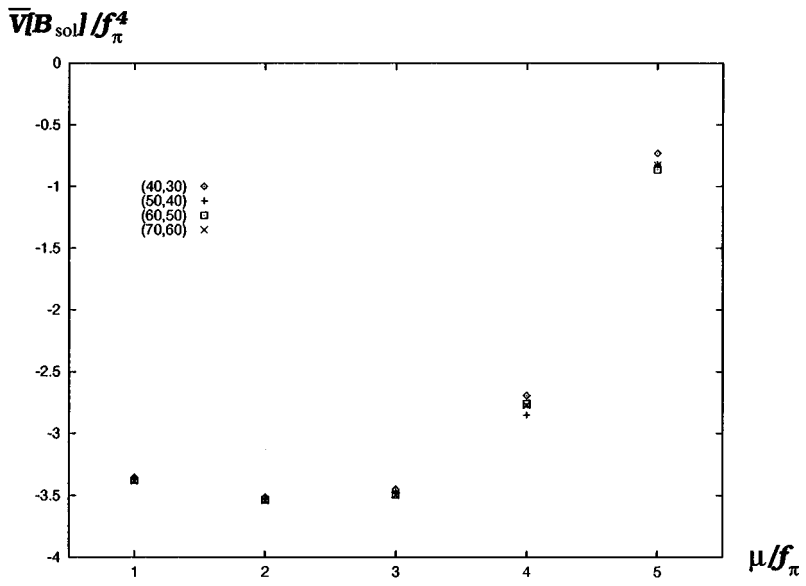

FIG. 4. Typical values of $\overline{V}[B_{\rm sol}]/f_\pi^4$ for four choices of the size of descretization, $(N_U,N_X)=(40,30)$, $(50,40)$, $(60,50)$, and $(70,60)$.

(4.4). To check the validity of the cutoffs in Eqs. (4.8) we show (a) the real part and (b) the imaginary part of the solution in Fig. 1, and integrands of (a) $f_\pi^2(\mu)$, (b) $-\overline{V}[B_{\rm sol}]$ in Fig. 2, at $\mu/f_\pi=3.0$ for $(N_U,N_X)=(70,60)$ by using the initial trial function (A). Figure 1(a) shows that the real part becomes small above $\Lambda_{\rm qcd}$. This behavior is similar to that of the solution at $T=\mu=0$. The dependence on x of the imaginary part is similar to that of the real part. Since the imaginary part is an odd function in u, it becomes zero in the infrared region of u. Figure 2 shows that the dominant part of each integrand lies within the integration range. These imply that the choice of range in Eqs. (4.8) is enough.

Next let us study the dependence of the results on the size of descretization. We show typical values of $f_\pi(\mu)/f_\pi$ in Fig. 3 and that of $\overline{V}[B_{\rm sol}]/f_\pi^4$ in Fig. 4 for four choices of the size of descretization, $(N_U,N_X)=(40,30)$, $(50,40)$, $(60,50)$, and $(70,60)$. This shows that the choice $(N_U,N_X)=(70,60)$ is large enough for the present purpose.

Now we show the resultant values of $f_\pi(\mu)/f_\pi$ for two choices of initial trial functions in Fig. 5. Below $\mu/f_\pi=3.0$ both trial functions converge to the same nontrivial solution. The value of $f_\pi(\mu)$ increases slightly. Choice (B) in Eqs. (4.9) converges to the trivial solution above $\mu/f_\pi=3.0$. However, the trial function (A) converges to a nontrivial solution, and the resultant value of $f_\pi(\mu)$ increases. Above $\mu/f_\pi=6.8$, (A) also converges to the trivial solution. In the range $3.0\leqslant\mu/f_\pi\leqslant6.8$ two initial trial functions converge to different solutions: one corresponds to the chiral broken

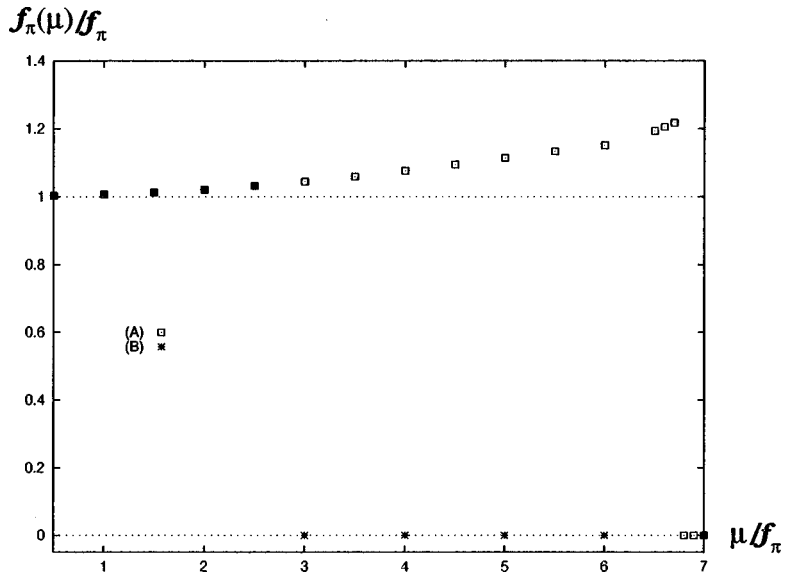

FIG. 5. μ dependence of $f_\pi(\mu)/f_\pi$ at $T=0$ for two choices of the initial trial functions (A) and (B) in Eq. (4.9).

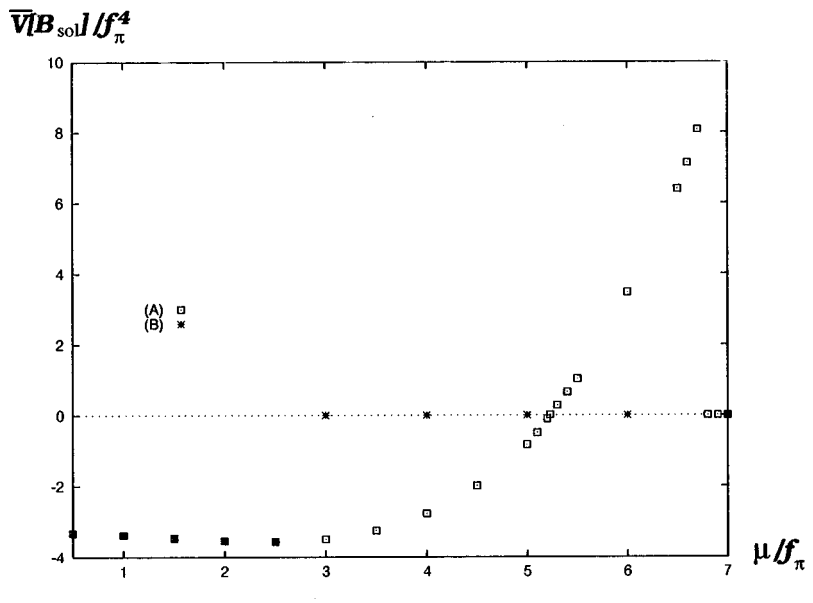

FIG. 6. μ dependence of the effective potential $\overline{V}[B_{\rm sol}]/f_\pi^4$ at $T=0$.

vacuum and another to the symmetric vacuum. Moreover, the trivial solution is always a solution of the SDE (2.15). Then we have to study which of the vacua is the true vacuum.

As we discussed in Sec. II, the true vacuum is determined by studying the effective potential. We show the value of the effective potential $\overline{V}[B_{\rm sol}]/f_\pi^4$ in Fig. 6. Since the value for the trivial solution is already subtracted from the expression in Eq. (2.18), a positive (negative) value of $\overline{V}[B_{\rm sol}]$ implies that the energy of the chiral broken vacuum is larger (smaller) than that of the symmetric vacuum. For $3.0 \leqslant \mu/f_\pi < 5.23$, $\overline{V}[B_{\rm sol}]_{(A)} < \overline{V}[B_{\rm sol}]_{(B)} = 0$, which implies that the chiral broken vacuum is energetically favored. On the other hand, for $5.23 \leqslant \mu/f_\pi \leqslant 6.8$, $\overline{V}[B_{\rm sol}]_{(A)} > 0$, and the chiral symmetric vacuum is the true vacuum. Chiral symmetry is restored at the point where the value of $\overline{V}[B_{\rm sol}]$ becomes positive: the chiral phase transition occurs at $\mu = 460$ MeV ($\mu/f_\pi = 5.23$). Since the value of the pion decay constant vanishes discontinuously at that point, the phase transition is clearly of first order. The nontrivial solutions for $5.23 \leqslant \mu/f_\pi \leqslant 6.8$ correspond to metastable states, which were shown in Ref. [13] by assuming a momentum dependence of the mass function. The result here obtained by solving the SDE (2.15) agrees qualitatively with their result.

C. $T \neq 0$ and $\mu = 0$

At nonzero temperature we perform the Matsubara frequency sum by truncating it at some finite number. Integra-

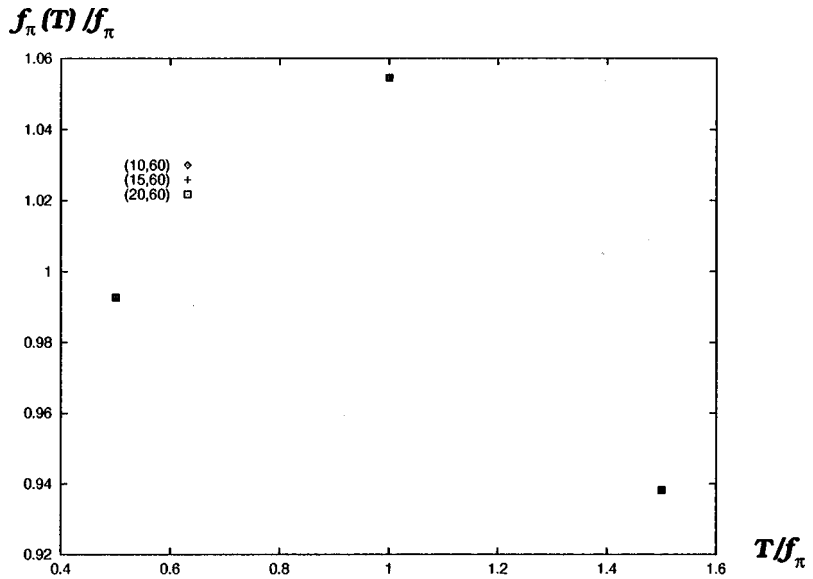

FIG. 7. Values of $f_\pi(T)/f_\pi$ at $T/f_\pi = 0.5$, 1.0, and 1.5 for three choices of the truncation point: $N_U = 10$, 15, and 20.

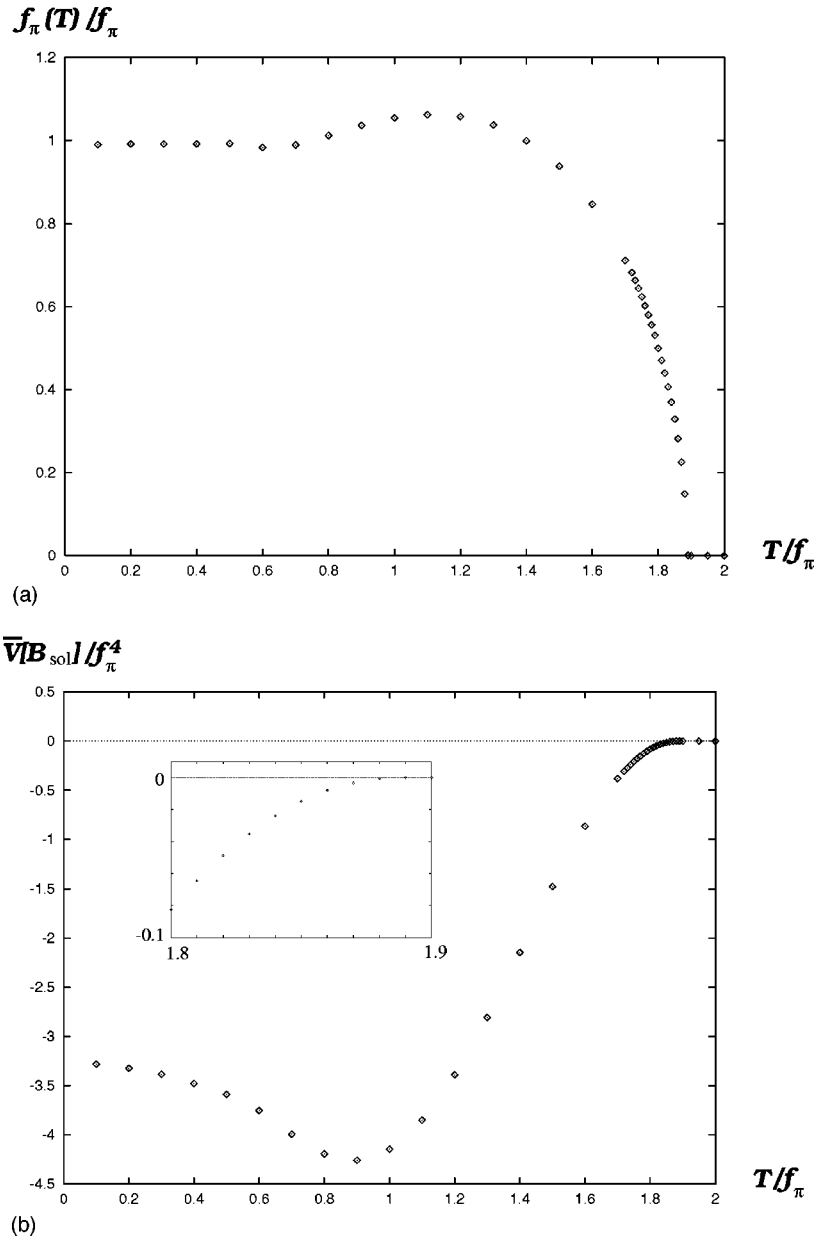

FIG. 8. Temperature dependences of (a) $f_\pi(T)/f_\pi$ and (b) $\overline{V}[B_{\rm sol}]/f_\pi^4$.

tion over the spatial momentum is done as shown in Eqs. (4.1) and (4.2). We have checked that the integration range given in the first line of Eqs. (4.8) is large enough for the present purpose. Since the trial function (B) converges to the same solution as (A) for small μ in the case of $T=0$, it may be enough to use the trial function (A) for studying the phase structure. Here and henceforth we use the trial function of type (A) only. First, we check the dependences of the results on the truncation. In Fig. 7 we show the values of $f_\pi(T)/f_\pi$ at $T/f_\pi=0.5$, 1.0, and 1.5 for three choices of the truncation point: $N_U=10$, 15, and 20. It is clear that the choice N_U $N_U=20$ is large enough as the truncation point for the present purpose.

The resultant temperature dependences of $f_\pi(T)/f_\pi$ and $\overline{V}[B_{\rm sol}]/f_\pi^4$ are shown in Fig. 8. The value of $f_\pi(T)$ does not change in the low temperature region. It increases once around $T/f_\pi\sim 0.7$ and decreases to zero above that point, and finally reaches zero around $T/f_\pi=1.89$. Differently from the previous case, the value of the potential reaches zero around the temperature where the decay constant vanishes. Since there are numerical errors in the present analysis, we cannot clearly show whether the decay constant and the potential vanish simultaneously. Our result shows that the chiral phase transition is of second order or of very weak first order, and that the critical temperature is around $T_c=166$ MeV.

D. $T\neq 0$ and $\mu\neq 0$

Now, we solve the SDE when both T and μ are nonzero. Infrared and ultraviolet cutoffs for x integration are fixed as

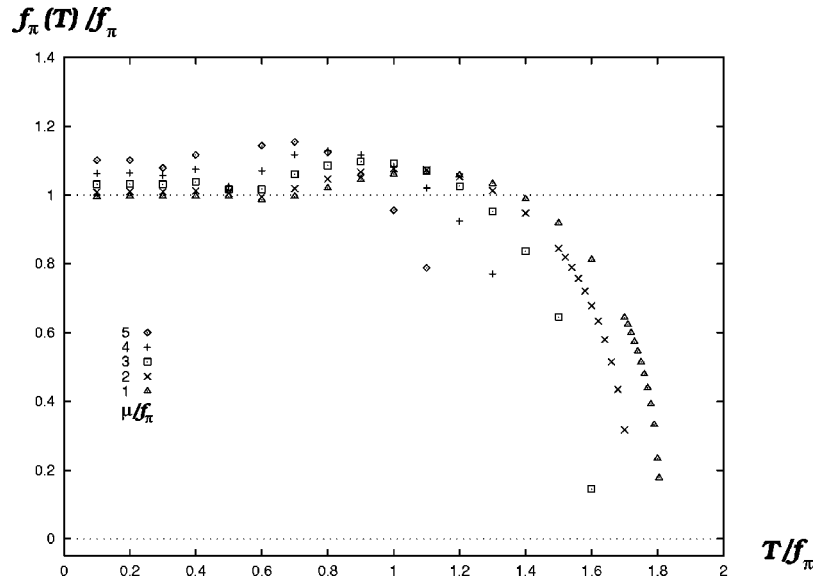

FIG. 9. Temperature dependences of $f_\pi(T)/f_\pi$ for $\mu/f_\pi=1$, 2, 3, 4, and 5.

in the first equation of Eqs. (4.8), and the sizes of descretizations are fixed to be $(N_U,N_X)=(20,60)$.

In the previous subsections we found that the phase transition at $T=0$ and $\mu\neq 0$ is of first order, while that at $T\neq 0$ and $\mu=0$ is of second order or of very weak first order. Then one can expect phase transitions of first order for small T and large μ, and those of weak first order for large T and small μ. First, we show the temperature dependence of $f_\pi(T)/f_\pi$ in Fig. 9 and that of $\overline{V}[B_{\rm sol}]/f_\pi^4$ in Fig. 10 for $\mu/f_\pi=1$, 2, 3, 4, and 5. Figure 9 shows that in all the cases the values of the pion decay constant increase once around $T\sim f_\pi$ and decrease above that. These, especially for $\mu/f_\pi=1$ and 2, behave as if the phase transitions are of second order. However, it is clear from Fig. 10 that the values of the effective potential $\overline{V}[B_{\rm sol}]$ become positive before the values of the pion decay constant vanish. Then the phase transitions are clearly of first order as in the case of $T=0$ and $\mu\neq 0$. To study phase transitions for smaller μ we concentrate on the temperature dependences around the phase transition points. Shown in Figs. 11 and 12 are the temperature dependences of the pion decay constant and the effective potential for $\mu/f_\pi=0.25$, 0.5, and 0.75 together with those for $\mu/f_\pi=1$. For $\mu/f_\pi=0.5$, 0.75, and 1.0 the values of the pion decay constant approach zero as if the phase transitions are of second order. However, the values of the effective potential become positive before the values of the decay constant reaches zero. Then we conclude that the phase transitions for $\mu/f_\pi=0.5$, 0.75, and 1.0 are clearly of first order. On the other hand, the phase transition for $\mu/f_\pi=0.25$ is of second order or of very weak first order.

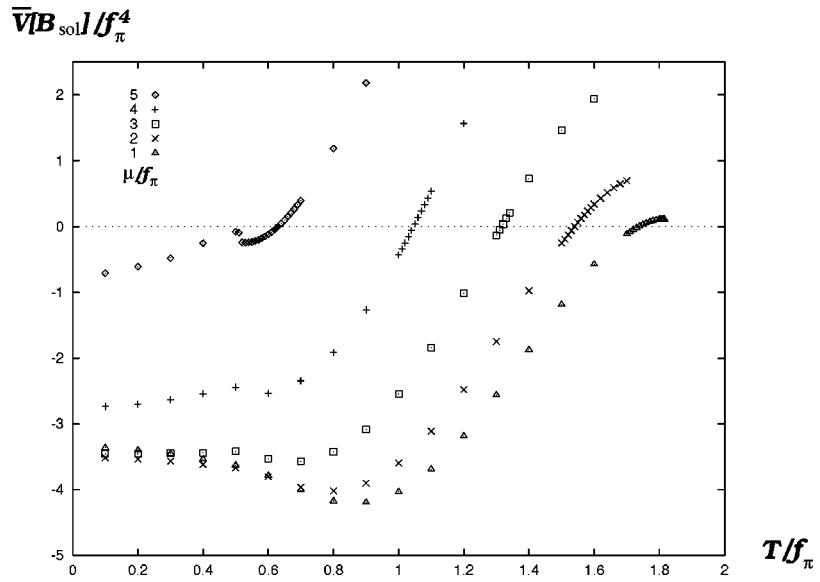

FIG. 10. Temperature dependence of the effective potential $\overline{V}[B_{\rm sol}]/f_\pi^4$ for $\mu/f_\pi=1$, 2, 3, 4, and 5.

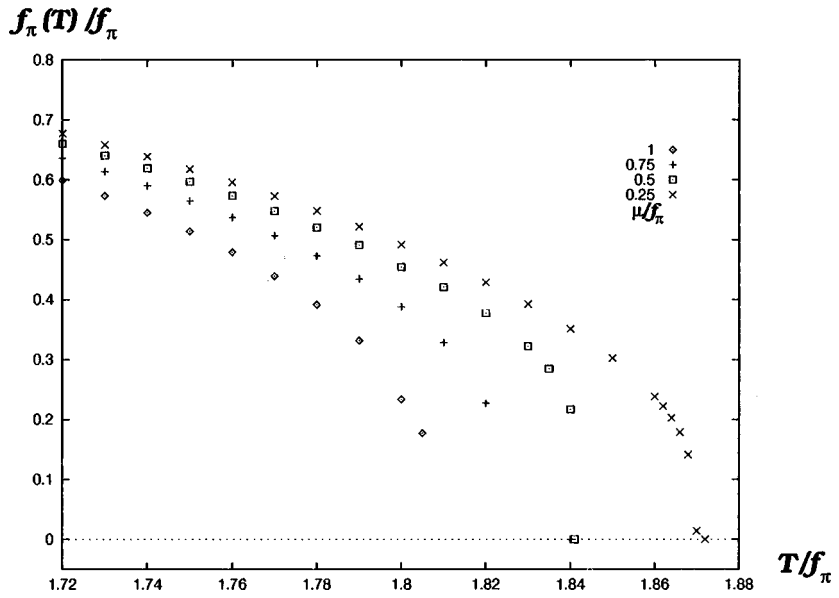

FIG. 11. Temperature dependences of $f_\pi(T)/f_\pi$ for $\mu/f_\pi=0.25$, 0.5, 0.75, and 1.0.

Finally we show a phase diagram derived by the present analysis in Fig. 13. As was expected, the phase transitions for small T and large μ are of first order, and those for large T and small μ are of second order or of very weak first order.

V. SUMMARY AND DISCUSSION

We analyzed the phase structure of QCD at finite temperature and density by solving the self-consistent Schwinger-Dyson equation for the quark propagator with the improved ladder approximation in the Landau gauge. A pion decay constant was calculated by using a generalized version of the Pagels-Stokar formula. The chiral phase transition point was determined by an effective potential for the propagator. When we raised the chemical potential μ with $T=0$, the value of the effective potential for the broken vacuum became bigger than that for the symmetric vacuum before the value of the pion decay constant vanished. The phase transition is clearly of first order. On the other hand, for $T\neq 0$ and $\mu=0$ the value of the effective potential for the broken vacuum reached that for the symmetric vacuum around the temperature where the value of the pion decay constant vanished. The phase transition is of second order or very weak first order. We presented the resultant phase diagram on a general T-μ plane. Phase transitions are clearly of first order in most cases, and for small μ they are of second order or very weak first order. Our results show that it is important to use the effective potential to study the phase structure at finite temperature and density.

Finally, some comments are in order. Generally the run-

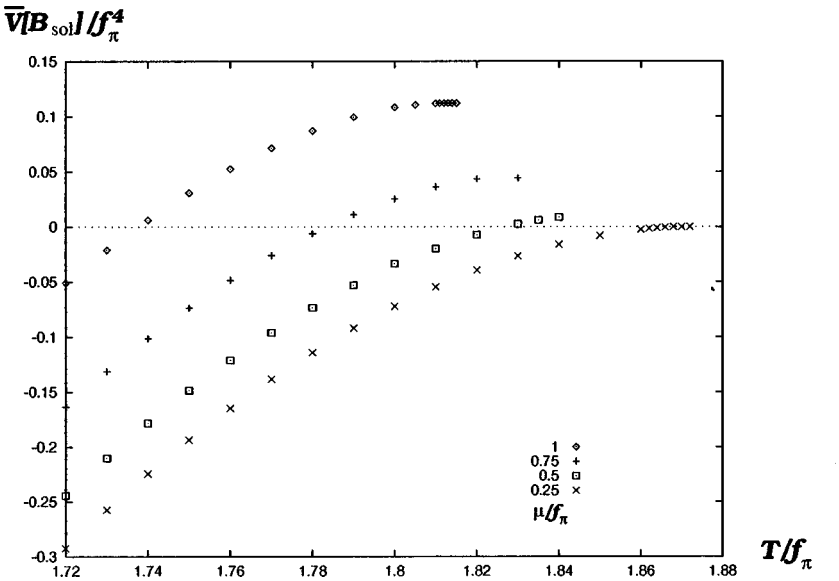

FIG. 12. Temperature dependence of the effective potential $\overline{V}[B_{\rm sol}]/f_\pi^4$ for $\mu/f_\pi=0.25$, 0.5, 0.75, and 1.0.

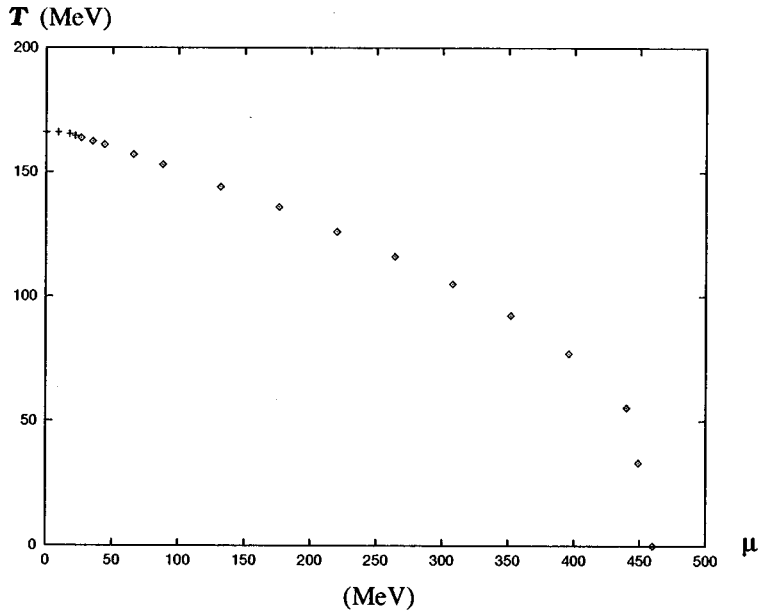

FIG. 13. Phase diagram obtained by the present analysis. Points indicated by ◇ are the phase transition points of first order and points by + of second order or very weak first order.

ning coupling should include the term from vacuum polarization of quarks and gluons at finite temperature and density. Moreover, the gluons at high temperature acquire an electric screening mass of order gT [28]. We dropped these effects, and used a running coupling and a gluon propagator of the same forms at $T=\mu=0$. (The same approximation was used in Ref. [17].) These effects can be included by using different running couplings and gluon propagators which depend explicitly on T and μ such as in Refs. [13,16].

The approximation of $A-1=C=0$ might not be good for high tempreture and/or density. However, inclusion of the deviations of $A-1$ and C from zero requires a large number for truncating the Matsubara frequency, and it is not efficient to apply the method used in this paper. A new method to solve the SDE may be needed. We expect that the inclusion of the deviations of $A-1$ and C from zero does not change the structure of the phase transition shown in the present paper.

ACKNOWLEDGMENTS

We would like to thank Professor Paul Frampton, Professor Taichiro Kugo, Professor Jack Ng, Professor Ryan Rohm, and Professor Joe Schechter for useful discussions and comments.

[1] R. D. Pisarski, BNL Report No. RP=941, hep-ph/9503330; G. E. Brown and M. Rho, Phys. Rep. **269**, 333 (1996); T. Hatsuda, H. Shiomi, and H. Kuwabara, Prog. Theor. Phys. **95**, 1009 (1996).

[2] T. Kugo, in *Proceedings of 1991 Nagoya Spring School on Dynamical Symmetry Breaking*, Nagoya, Japan, 1991, edited by K. Yamawaki (World Scientific, Singapore, 1991); V. A. Miransky, *Dynamical Symmetry Breaking in Quantum Field Theory* (World Scientific, Singapore, 1993).

[3] C. De Dominicis and P. C. Martin, J. Math. Phys. **5**, 14 (1964); **5**, 31 (1964).

[4] J. M. Cornwall, R. Jackiw, and E. Tomboulis, Phys. Rev. D **10**, 2428 (1974).

[5] For a review, see, e.g., R. W. Haymaker, Nuovo Cimento **14**, 1 (1991), and references therein.

[6] M. Bando, M. Harada, and T. Kugo, Prog. Theor. Phys. **91**, 927 (1994).

[7] O. K. Kalashnikov, Pis'ma Zh. Éksp. Teor. Fiz. **41**, 477 (1985) [JETP Lett. **41**, 153 (1985)].

[8] J. Cleymans, R. V. Gavai, and E. Suhonen, Phys. Rep. **130**, 217 (1986).

[9] R. Gupta, G. Guralnik, G. W. Kilcup, A. Patel, and S. R. Shape, Phys. Rev. Lett. **57**, 2621 (1986).

[10] T. Akiba, Phys. Rev. D **36**, 1905 (1987).

[11] O. K. Kalashnikov, Z. Phys. C **39**, 427 (1988).

[12] A. Cabo, O. K. Kalashnikov, and E. Kh. Veliev, Nucl. Phys. **B299**, 367 (1988).

[13] A. Barducci, R. Casalbuoni, S. De Curtis, R. Gatto, and G. Pettini, Phys. Rev. D **41**, 1610 (1990).

[14] A. Barducci, R. Casalbuoni, S. De Curtis, R. Gatto, and G. Pettini, Phys. Lett. B **240**, 429 (1990).
[15] S. D. Odintsov and Yu. I. Shil'nov, Mod. Phys. Lett. A **6**, 707 (1991).
[16] K.-I. Kondo and K. Yoshida, Int. J. Mod. Phys. A **10**, 199 (1995).
[17] Y. Taniguchi and Y. Yoshida, Phys. Rev. D **55**, 2283 (1997).
[18] D.-S. Lee, C. N. Leung, and Y. J. Ng, Phys. Rev. D **55**, 6504 (1997); **57**, 5224 (1998); V. P. Gusynin and I. A. Shovkovy, *ibid.* **56**, 5251 (1997); P. Maris, C. D. Roberts, and P. C. Tandy, Phys. Lett. B **420**, 267 (1998); D. Blashke, C. D. Roberts, and S. Schmidt, *ibid.* **425**, 232 (1998); A. Bender, G. I. Poulis, C. D. Roberts, S. Schmidt, and A. W. Thomas, *ibid.* **431**, 263 (1998).
[19] H. Pagels and S. Stokar, Phys. Rev. D **20**, 2947 (1979).
[20] T. Matsubara, Prog. Theor. Phys. **14**, 351 (1955).
[21] T. Toimele, Int. J. Theor. Phys. **24**, 901 (1985).
[22] J. Kapusta, *Finite-Temperature Field Theory* (Cambridge University Press, Cambridge, England, 1989).
[23] T. Kugo and M. Mitchard, Phys. Lett. B **282**, 162 (1992); **286**, 355 (1992).
[24] K.-I. Aoki, M. Bando, T. Kugo, M. G. Mitchard, and H. Nakatani, Prog. Theor. Phys. **84**, 683 (1990).
[25] R. D. Pisarski and M. Tytgat, Phys. Rev. D **54**, R2989 (1996).
[26] M. Tanabashi, in *Proceedings of 1991 Nagoya Spring School on Dynamical Symmetry Breaking* [2].
[27] J. Gasser and H. Leutwyler, Ann. Phys. (N.Y.) **158**, 142 (1984).
[28] K. Kajantie and J. Kapusta, Ann. Phys. (N.Y.) **160**, 477 (1985).